Journal of Magnetic Resonance **152,** 162–167 (2001)
doi:10.1006/jmre.2001.2395, available online at http://www.idealibrary.com on IDEAL®

Two-Dimensional NMR of Velocity Exchange: VEXSY and SERPENT

B. Blümich,* P. T. Callaghan,† R. A. Damion,‡,§ S. Han,* A. A. Khrapitchev,† K. J. Packer,‡ and S. Stapf*,[1]

**Lehrstuhl für Makromolekulare Chemie, ITMC, RWTH Aachen, Worringerweg 1, D-52074 Aachen, Germany; †Institute of Fundamental Sciences–Physics, Massey University, Palmerston North, New Zealand; ‡Department of Chemistry, University of Nottingham, University Park, Nottingham NG7 2RD, United Kingdom; and §School of Mathematical Sciences, University of Nottingham, University Park, Nottingham NG7 2RD, United Kingdom*

Received February 14, 2001; revised May 29, 2001; published online August 1, 2001

Two different multidimensional pulsed field gradient sequences are compared which have the purpose of correlating spin displacements in different time intervals with each other. The simplest possible sequence, three-pulse SERPENT, measures displacements in two interleaved time intervals, while in VEXSY, consisting of two independent pairs of gradient pulses separated by a mixing time, displacements during the two encoding intervals are compared to each other. The formalism for both sequences is discussed in q space and in displacement space and common features as well as differences between the two types of experiments are highlighted, employing the particular case of the concurrent VEXSY scheme which allows treatment according to both formalisms. © 2001 Academic Press

Key Words: **PFG; displacements; correlations; 2D; flow.**

INTRODUCTION

In 1993 Callaghan and Manz proposed a new type of pulsed gradient spin-echo experiment in which two independent pairs of gradient pulses were used to encode for nuclear spin displacement over two separated, but well-defined, time intervals (*1*). This two-dimensional NMR spectroscopy method, known as VEXSY (Velocity EXchange SpectroscopY), was in the form of a classical NMR exchange experiment, which is used to find correlations between features in the frequency spectrum by the identification of cross-signals in a two-dimensional density representation $S(f_1, f_2)$ (*2–4*). In VEXSY, the displacements (or velocities) for each molecule in the macroscopic ensemble are compared at two different times. The domains equivalent to f_1 and f_2 in classical spectroscopy correspond to the displacements $\mathbf{R}_1$ and $\mathbf{R}_2$ over two identical encoding intervals, which are themselves separated by a further time delay, τ_m, the equivalent of the "mixing" time in the conventional exchange experiment. The conjugate "preparation" and "detection" domains correspond to the $\mathbf{q}$ space of the pulsed gradient spin-echo (PGSE) method (*5, 6*). The PGSE gradient pulse pairs are stepped so as to phase-encode the spins for molecular translational motion. Both pairs of field gradient pulses independently define a value of $\mathbf{q}$. They are usually applied in the same spatial direction so that a spin isochromat corresponding to a set of molecules traveling at constant velocity will have identical $\mathbf{R}_1$ and $\mathbf{R}_2$ displacements, thus contributing to points on the diagonal in $(\mathbf{R}_1, \mathbf{R}_2)$ space. By contrast, a migration of spins from one region of the displacement spectrum to another over the time τ_m will lead to off-diagonal contributions. In this manner the molecular velocities may be correlated. Application of VEXSY, mainly to fluid flow and particle motion problems, has seen an increasing literature in recent years and the interpretation of such correlations has been discussed by means of coordinate transformations (*7–9*) and suitable 1D-experiments (*10–15*).

In 1999 an apparently different pulsed gradient spin-echo experiment was proposed by Stapf *et al.* (*16*), in which an arbitrary number of sequential gradient pulses is applied to the spin ensemble, each with an arbitrary amplitude, but with the requirement that the time integral of the gradient waveforms over the whole experiment be zero, which is the condition required for echo formation. (Note that the additional influence of background gradients will be neglected throughout this paper.) The encoding of position, starting with the first gradient pulse, is thus followed by a repeated labeling of the particles at the times of each successive gradient pulse so that the statistics of motion become encoded into the echo signal acquired after completion of the sequence. In its simplest realization, i.e., three successive gradient pulses, the echo constraint determines that two gradient pulses may be independently varied, thus implying a two-dimensional encoding space. This experiment was termed SERPENT for SEquential Rephasing by Pulsed field gradients Encoding N Time intervals (*16, 17*). Both VEXSY and SERPENT belong to a family of PFG sequences which employ a multiple encoding of spin position but retain only displacement information due to the fact that the echo condition is fulfilled at the end of the sequence. Both experiments apparently measure joint probabilities for displacements $\mathbf{R}_1$ and $\mathbf{R}_2$ over two different time intervals. We shall show here that in fact the three-pulse SERPENT and the VEXSY experiments contain precisely the same information, albeit with ostensibly different coordinates. The interpretation of this information, however, depends on the

[1] To whom correspondence should be addressed at Lehrstuhl für Makromolekulare Chemie, ITMC, RWTH Aachen, Worringerweg 1, D-52074 Aachen, Germany. Fax: +49-241-8888-185. E-mail: sstapf@mc.rwth-aachen.de.

1090-7807/01 $35.00

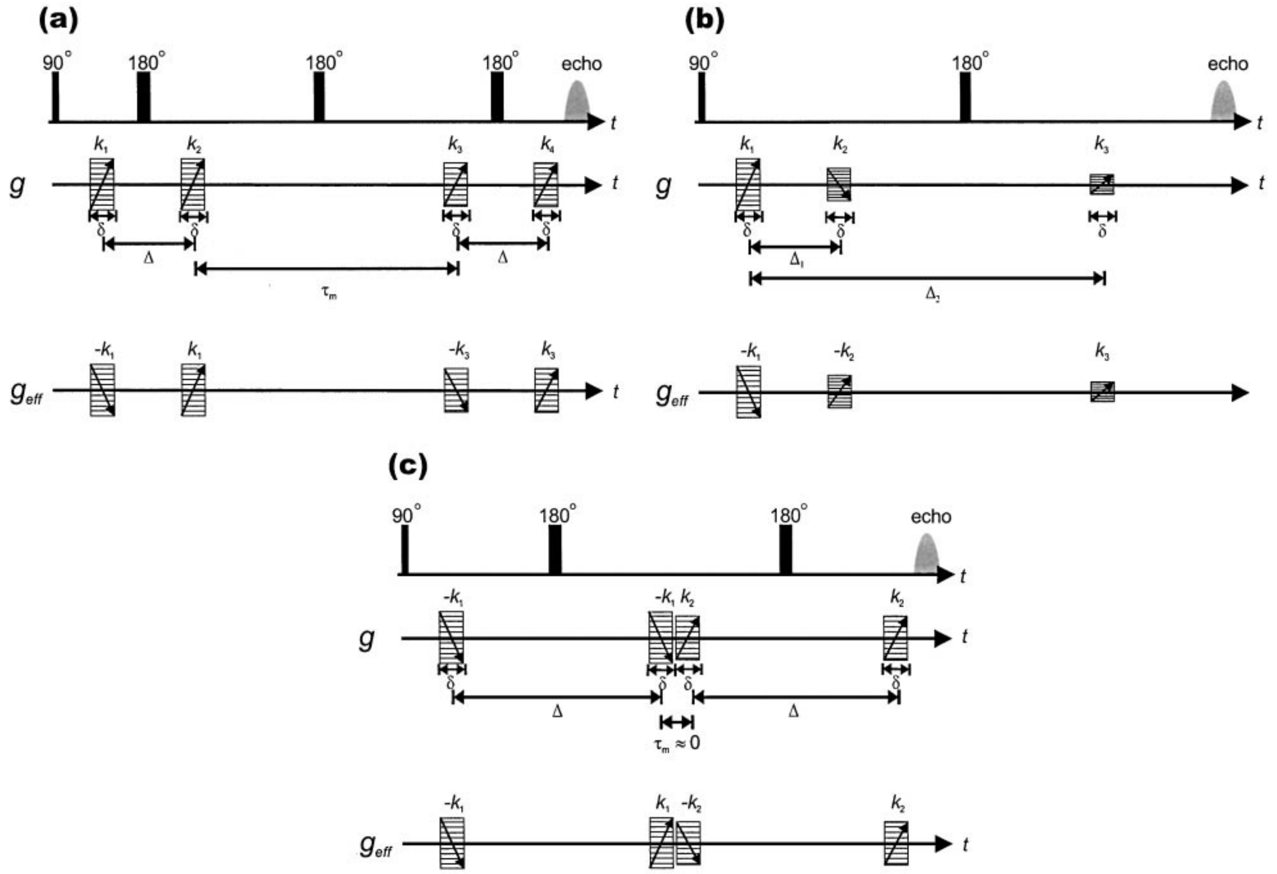

FIG. 1. (a) Spin-echo pulse sequence to encode displacements during two identical time intervals, Δ (VEXSY). Both gradient pairs of wave vectors $\mathbf{k}_1 = -\mathbf{k}_2$ and $\mathbf{k}_3 = -\mathbf{k}_4$ are stepped independently of each other. The mixing time τ_m is measured between the second and the third gradient pulse. (b) Spin-echo pulse sequence to encode displacements during two overlapping time intervals, Δ_1 and Δ_2 (SERPENT). The gradients of wave vectors $\mathbf{k}_2$ and $\mathbf{k}_3$ are stepped independently of each other and $\mathbf{k}_1$ is computed subject to the condition that the sum of the effective gradients is zero. (c) VEXSY spin-echo pulse sequence according to (a) with vanishing mixing time. The second and third gradient pulses can be concatenated into a single pulse. Below each sequence with RF pulses is shown the effective gradient equivalent where each 180° RF pulse is replaced by an inversion of the sign of the gradient wave vector.

choice of encoding times, as well as the wave vectors with respect to which Fourier transformation is performed, and allows focusing on either an integral or a differential aspect of fluid motion.

The respective pulse sequences for VEXSY and SERPENT are compared in Figs. 1a and 1b. Figure 1c presents a concatenated version of VEXSY which we shall show is essentially equivalent to SERPENT. In each figure we show first a spin-echo version using RF pulses, and then, below, the effective gradient equivalent (in which 180° RF pulses have the effect of inverting the sign of the prior gradient pulses). For convenience we employ the usual definition $\mathbf{k} = (2\pi)^{-1}\gamma\mathbf{g}\delta$ where $\mathbf{g}\delta$ is the area under the gradient pulse.

We first analyze the respective pulse sequences using the established language of propagators, making clear which probability densities each method is able to measure. By example of a special case which can be described by either terminology, we compare the salient features of both sequences with each other. We conclude by commenting on the applicability of both methods depending on the main interest of the experimental problem.

THE PROPAGATOR FORMALISM

The propagator analysis for each pulse sequence is illustrated with the help of Fig. 1 as follows: In the VEXSY experiment (Fig. 1a), the four gradient pulses with wave vectors $\mathbf{k}_1, \mathbf{k}_2, \mathbf{k}_3, \mathbf{k}_4$ are applied in pairs, each of which meets the echo condition; thus $\mathbf{k}_1 + \mathbf{k}_2 = 0$ and $\mathbf{k}_3 + \mathbf{k}_4 = 0$. The effective gradient pulses along with their time separations are then given by $(-\mathbf{k}_1)$–Δ–$(\mathbf{k}_1)$–τ_m–$(-\mathbf{k}_3)$–Δ–$(\mathbf{k}_3)$. For an oppositely directed pair of pulses, $\mathbf{k}_i$ and $-\mathbf{k}_i$, $\mathbf{q}_i = (\mathbf{k}_i - (-\mathbf{k}_i))/2$ or, in other words $\mathbf{q}_i = \mathbf{k}_i$. The pairs $(-\mathbf{k}_1)$–Δ–$(\mathbf{k}_1)$ and $(-\mathbf{k}_3)$–Δ–$(\mathbf{k}_3)$ define scattering wave vectors $\mathbf{q}_1$ and $\mathbf{q}_3$, respectively. We now formulate the expression for the echo attenuation in terms of the wave vectors, $\mathbf{k}$, and the position vectors, $\mathbf{r}$. From

$$E(\mathbf{k}_1,\mathbf{k}_2,\mathbf{k}_3,\mathbf{k}_4)=\iiiint\rho(\mathbf{r}_1)\exp(-i2\pi\mathbf{k}_1\mathbf{r}_1)P(\mathbf{r}_1\mid\mathbf{r}_2,\Delta)\times\exp(-i2\pi\mathbf{k}_2\mathbf{r}_2)P(\mathbf{r}_2\mid\mathbf{r}_3,\tau_\mathrm{m})\times\exp(-i2\pi\mathbf{k}_3\mathbf{r}_3)P(\mathbf{r}_3\mid\mathbf{r}_4,\Delta)\times\exp(-i2\pi\mathbf{k}_4\mathbf{r}_4)\,d\mathbf{r}_1\,d\mathbf{r}_2\,d\mathbf{r}_3\,d\mathbf{r}_4 \qquad [1]$$

we then obtain the echo amplitude

$$E(\mathbf{k}_1,\mathbf{k}_3)=\iiiint\rho(\mathbf{r}_1)\exp(-i2\pi\mathbf{k}_1\mathbf{r}_1)P(\mathbf{r}_1\mid\mathbf{r}_2,\Delta)\times\exp(i2\pi\mathbf{k}_1\mathbf{r}_2)P(\mathbf{r}_2\mid\mathbf{r}_3,\tau_\mathrm{m})\exp(-i2\pi\mathbf{k}_3\mathbf{r}_3)\times P(\mathbf{r}_3\mid\mathbf{r}_4,\Delta)\exp(i2\pi\mathbf{k}_3\mathbf{r}_4)\,d\mathbf{r}_1\,d\mathbf{r}_2\,d\mathbf{r}_3\,d\mathbf{r}_4, \qquad [2]$$

where $\rho(\mathbf{r}_1)$ is the initial spin density distribution, $\mathbf{r}_n$ is the nuclear spin position at the time of the nth gradient pulse, and the $P(\mathbf{r}_n\mid\mathbf{r}_m,t)$ are conditional probabilities for a particle initially at $\mathbf{r}_n$ to move to $\mathbf{r}_m$ over time t. The underlying assumption is that the duration of the gradient pulses δ is short ($\delta\ll\Delta$), and that motions during δ can be neglected.

The equation above is expressed in a four-dimensional coordinate system, ($\mathbf{r}_1$, $\mathbf{r}_2$, $\mathbf{r}_3$, $\mathbf{r}_4$) which denotes positions at the times t_1, t_2, t_3, t_4 when the gradient pulses are applied. Rewriting the equation in terms of a new set of independent variables defined by

$$\mathbf{r}_1,\quad \mathbf{R}_1=\mathbf{r}_2-\mathbf{r}_1,\quad \mathbf{R}_2=\mathbf{r}_3-\mathbf{r}_2,\quad \mathbf{R}_3=\mathbf{r}_4-\mathbf{r}_3, \qquad [3]$$

where the $\mathbf{R}$ vectors represent successive displacements, we define for equal magnitudes of the gradient pulses in the first pulse pair ($\mathbf{q}_1$) as well as in the second pulse pair ($\mathbf{q}_3$)

$$E(\mathbf{q}_1,\mathbf{q}_3)=\iiiint\rho(\mathbf{r}_1)P(\mathbf{r}_1\mid\mathbf{r}_1+\mathbf{R}_1,\Delta)P(\mathbf{r}_1+\mathbf{R}_1\mid\mathbf{r}_1+\mathbf{R}_1+\mathbf{R}_2,\tau_\mathrm{m})P(\mathbf{r}_1+\mathbf{R}_1+\mathbf{R}_2\mid\mathbf{r}_1+\mathbf{R}_1+\mathbf{R}_2+\mathbf{R}_3,\Delta)\,d\mathbf{r}_1\,d\mathbf{R}_2\exp\{i2\pi(\mathbf{q}_1\mathbf{R}_1+\mathbf{q}_3\mathbf{R}_3)\}\times d\mathbf{R}_1\,d\mathbf{R}_3$$
$$:=\iint\bar{P}(\mathbf{R}_1,\Delta)\mathcal{P}_\mathrm{V}(\mathbf{R}_1,\Delta\mid\mathbf{R}_3,\Delta;\tau_\mathrm{m})\times\exp\{i2\pi(\mathbf{q}_1\mathbf{R}_1+\mathbf{q}_3\mathbf{R}_3)\}\,d\mathbf{R}_1\,d\mathbf{R}_3 \qquad [4]$$

where $\bar{P}(\mathbf{R}_1,\Delta)$ is the average propagator which describes the probability that a particle displaces by $\mathbf{R}_1$ over time Δ independent of the starting position (*6, 18*) while $\mathcal{P}_\mathrm{V}(\mathbf{R}_1,\ \Delta\mid\mathbf{R}_3,\ \Delta;\ \tau_\mathrm{m})$ is the conditional probability that, if a displacement by $\mathbf{R}_1$ occurs during the first interval Δ, then a displacement $\mathbf{R}_3$ will occur during the third time interval of equal duration to the first, delayed by a mixing time τ_m. This particular nomenclature has been chosen to emphasize that $\mathcal{P}_\mathrm{V}$ describes the conditional probability between *displacements* in the VEXSY case, hence the subscript V, as compared to $P(\mathbf{r}_n|\mathbf{r}_m,t)$ which relates *positions* to each other. Note that in Eq. [4] one integrates not only over the starting position $\mathbf{r}_1$ but also over the displacement $\mathbf{R}_2$ accumulated during τ_m between the encoding gradient pairs, so that information about $\mathbf{R}_2$ is effectively averaged out.

Normally the gradient pulses are applied along a single direction (the z axis) and the data collected in two dimensions, (q_1, q_3). Then, inverse Fourier transformation with respect to (q_1, q_3) returns the two-dimensional Fourier spectrum

$$S(Z_1,Z_3)=\bar{P}(Z_1,\Delta)\mathcal{P}_\mathrm{V}(Z_1,\ \Delta\mid Z_3,\ \Delta;\ \tau_\mathrm{m}). \qquad [5]$$

In the special case of a velocity distribution where spins are not allowed to change their individual velocity, such as laminar flow in the absence of self-diffusion, $\mathcal{P}_\mathrm{V}(Z_1,\ \Delta\mid Z_3,\ \Delta;\ \tau_\mathrm{m})$ is the Dirac delta function $\delta(Z_1-Z_3)$ and the two-dimensional spectrum is diagonal,

$$S(Z_1,Z_3)=\bar{P}(Z_1,\Delta)\,\delta(Z_1-Z_3). \qquad [6]$$

SERPENT (FIG. 1b)

In analogy to the notation of Stapf *et al.* (*16*), the effective gradient pulses along with their time separations are $(-\mathbf{k}_1)$–Δ_1–$(-\mathbf{k}_2)$–$(\Delta_2-\Delta_1)$–$(\mathbf{k}_3)$, where $-\mathbf{k}_1-\mathbf{k}_2+\mathbf{k}_3=0$. The echo amplitude is given by

$$E(\mathbf{k}_1,\mathbf{k}_2,\mathbf{k}_3)=\iiint\rho(\mathbf{r}_1)\exp(-i2\pi\mathbf{k}_1\mathbf{r}_1)P(\mathbf{r}_1\mid\mathbf{r}_2,\Delta_1)\times\exp(-i2\pi\mathbf{k}_2\mathbf{r}_2)P(\mathbf{r}_2\mid\mathbf{r}_3,\Delta_2-\Delta_1)\times\exp(i2\pi\mathbf{k}_3\mathbf{r}_3)\,d\mathbf{r}_1\,d\mathbf{r}_2\,d\mathbf{r}_3. \qquad [7]$$

Rewriting in terms of a new set of independent variables defined by displacements $\mathbf{R}_1$ and $\mathbf{R}_2'$ from the initial position $\mathbf{r}_1$

$$\mathbf{r}_1,\quad \mathbf{R}_1=\mathbf{r}_2-\mathbf{r}_1,\quad \mathbf{R}_2'=\mathbf{r}_3-\mathbf{r}_1, \qquad [8]$$

one obtains

$$E(\mathbf{k}_2,\mathbf{k}_3)=\iiint\rho(\mathbf{r}_1)P(\mathbf{r}_1\mid\mathbf{r}_1+\mathbf{R}_1,\Delta_1)P(\mathbf{r}_1+\mathbf{R}_1\mid\mathbf{r}_1+\mathbf{R}_2',\Delta_2-\Delta_1)\,d\mathbf{r}_1\exp(i2\pi\mathbf{k}_2\mathbf{R}_1)\times\exp(i2\pi\mathbf{k}_3\mathbf{R}_2')\,d\mathbf{R}_1\,d\mathbf{R}_2' \qquad [9]$$

and

$$E(\mathbf{q}_2,\mathbf{q}_3):=\iint\bar{P}(\mathbf{R}_1,\Delta_1)\mathcal{P}_\mathrm{S}(\mathbf{R}_1,\Delta_1\mid\mathbf{R}_2',\ \Delta_2)\times\exp\{i2\pi(\mathbf{q}_2\mathbf{R}_1+\mathbf{q}_3\mathbf{R}_2')\}\,d\mathbf{R}_1\,d\mathbf{R}_2',$$

where for convenience we define $\mathbf{q}_2=\mathbf{k}_2$, $\mathbf{q}_3=\mathbf{k}_3$. $\mathcal{P}_\mathrm{S}(\mathbf{R}_1,\Delta_1\mid\mathbf{R}_2',\Delta_2)$ now describes the conditional probability that, if a displacement by $\mathbf{R}_1$ occurs during the first interval Δ_1, then a displacement $\mathbf{R}_2'$ will occur during the total time interval Δ_2

which incorporates Δ_1. Note that this representation is different from the function introduced for the VEXSY experiment, $\mathcal{P}_V(\mathbf{R}_1, \Delta \mid \mathbf{R}_3,\ \Delta;\ \tau_m)$, but is a consequence of the way the SERPENT experiment and the subsequent Fourier transformation are performed as will be shown in the under Comparison later in this paper.

Again, the gradient pulses are frequently applied along a single direction (the *z axis*) and the data collected in two dimensions, (q_2, q_3), although it is entirely possible for them to be in different directions. Then, inverse Fourier transformation with respect to (q_2, q_3) returns the two-dimensional Fourier spectrum

$$S(Z_1,\ Z_2') = \bar{P}(Z_1, \Delta_1)\, \mathcal{P}_S(Z_1, \Delta_1 \mid Z_2', \Delta_2). \qquad [10]$$

$S(Z_1,\ Z_2')$ is precisely the joint probability $W(Z_1, \Delta_1;\ Z_2', \Delta_2)$ discussed by Stapf *et al.* (*16*). Note that SERPENT produces a spectrum in which the displacements, $Z_1,\ Z_2'$, are plotted over two time intervals different from those of the VEXSY experiment. The second of these displacements incorporates the first. Thus in the event of a velocity distribution as discussed in Eq. [6], SERPENT will not return a diagonal two-dimensional spectrum but one which is inclined to the longer interval axis.

CONCURRENT VEXSY (FIG. 1c)

We now consider the VEXSY sequence in which the mixing time is set to zero, as shown in Fig. 1c. Now the effective gradient pulses along with their time separations are $(-\mathbf{k}_1)$–Δ–$(\mathbf{k}_1)\,(-\mathbf{k}_2)$–$\Delta$–$(\mathbf{k}_2)$. The adjacent pair $(\mathbf{k}_1)(-\mathbf{k}_2)$ can be concatenated to a single pulse $\mathbf{k}_1'$ where $\mathbf{k}_1' = \mathbf{k}_1 - \mathbf{k}_2$. This gives us the equivalent of the three-pulse SERPENT experiment in which the SERPENT triad $(\mathbf{k}_1, \mathbf{k}_2, \mathbf{k}_3)$ is now $(-\mathbf{k}_1, \mathbf{k}_1', \mathbf{k}_2)$ and, as required, sums to zero.

The normalized echo amplitude is given by

$$E(\mathbf{k}_1, \mathbf{k}_1',\ \mathbf{k}_2) = \iiint \rho(\mathbf{r}_1) \exp(-i2\pi \mathbf{k}_1 \mathbf{r}_1) P(\mathbf{r}_1 \mid \mathbf{r}_2, \Delta) \times \exp(i2\pi \mathbf{k}_1' \mathbf{r}_2) P(\mathbf{r}_2 \mid \mathbf{r}_3, \Delta) \exp(i2\pi \mathbf{k}_2 \mathbf{r}_3) \times d\mathbf{r}_1\, d\mathbf{r}_2\, d\mathbf{r}_3. \qquad [11]$$

One can now rewrite Eq. [11] following the VEXSY terminology, in terms of a new set of independent variables defined by successive displacements $\mathbf{R}_1$ and $\mathbf{R}_2$ from the initial position $\mathbf{r}_1$,

$$\mathbf{r}_1, \quad \mathbf{R}_1 = \mathbf{r}_2 - \mathbf{r}_1, \quad \mathbf{R}_2 = \mathbf{r}_3 - \mathbf{r}_2, \qquad [12]$$

and obtains

$$E(\mathbf{k}_1, \mathbf{k}_2) = \iiint \rho(\mathbf{r}_1) P(\mathbf{r}_1 \mid \mathbf{r}_1 + \mathbf{R}_1, \Delta) P(\mathbf{r}_1 + \mathbf{R}_1 \mid \mathbf{r}_1 + \mathbf{R}_1 + \mathbf{R}_2, \Delta)\, d\mathbf{r}_1 \exp(i2\pi \mathbf{k}_1 \mathbf{R}_1) \times \exp(i2\pi \mathbf{k}_2 \mathbf{R}_2)\, d\mathbf{R}_1\, d\mathbf{R}_2, \qquad [13]$$

$$E(\mathbf{q}_1, \mathbf{q}_2) := \iint \bar{P}(\mathbf{R}_1, \Delta) \mathcal{P}_V(\mathbf{R}_1, \Delta \mid \mathbf{R}_2, \Delta; 0) \times \exp\{i2\pi(\mathbf{q}_1 \mathbf{R}_1 + \mathbf{q}_2 \mathbf{R}_2)\}\, d\mathbf{R}_1\, d\mathbf{R}_2,$$

where $\mathbf{q}_1 = \mathbf{k}_1$, $\mathbf{q}_2 = \mathbf{k}_2$.

For gradient pulses which are applied along a single direction (the *z axis*) and with the data collected in two dimensions, (q_1, q_2), inverse Fourier transformation with respect to (q_1, q_2) returns the two-dimensional Fourier spectrum

$$S(Z_1, Z_2) = \bar{P}(Z_1, \Delta) \mathcal{P}_V(Z_1, \Delta \mid Z_2, \Delta; 0). \qquad [14]$$

Alternatively, one can assume the SERPENT terminology and rewrite in terms of a new set of independent variables defined by displacements $\mathbf{R}_1$ and $\mathbf{R}_2'$ from the initial position $\mathbf{r}_1$

$$\mathbf{r}_1, \quad \mathbf{R}_1 = \mathbf{r}_2 - \mathbf{r}_1, \quad \mathbf{R}_2' = \mathbf{r}_3 - \mathbf{r}_1, \qquad [15]$$

in which case one obtains

$$E(\mathbf{k}_1',\ \mathbf{k}_2) = \iiint \rho(\mathbf{r}_1) P(\mathbf{r}_1 \mid \mathbf{r}_1 + \mathbf{R}_1, \Delta_1) P(\mathbf{r}_1 + \mathbf{R}_1 \mid \mathbf{r}_1 + \mathbf{R}_2',\ \Delta_2 - \Delta_1)\, d\mathbf{r}_1 \exp(i2\pi \mathbf{k}_1' \mathbf{R}_1) \times \exp(i2\pi \mathbf{k}_2 \mathbf{R}_2')\, d\mathbf{R}_1\, d\mathbf{R}_2' \qquad [16]$$

$$E(\mathbf{q}_1',\ \mathbf{q}_2) := \iint \bar{P}(\mathbf{R}_1, \Delta_1) \mathcal{P}_S(\mathbf{R}_1, \Delta_1 \mid \mathbf{R}_2',\ \Delta_2) \times \exp\{i2\pi(\mathbf{q}_1' \mathbf{R}_1 + \mathbf{q}_2 \mathbf{R}_2')\}\, d\mathbf{R}_1\, d\mathbf{R}_2',$$

where $\mathbf{q}_1' = \mathbf{k}_1'$, $\mathbf{q}_2 = \mathbf{k}_2$. Inverse Fourier transformation with respect to (q_1', q_2) now returns the two-dimensional Fourier spectrum

$$S(Z_1, Z_2') = \bar{P}(Z_1, \Delta_1) \mathcal{P}_S(Z_1, \Delta_1 \mid Z_2', \Delta_2). \qquad [17]$$

In this special case, Eqs. [14] and [17] are two complementary representations of the same physical situation with $\Delta_1 = \Delta$ and $\Delta_2 = 2\Delta$, where $Z_2' = Z_1 + Z_2$.

COMPARISON OF VEXSY AND SERPENT

As has been described in the above paragraph, the two-dimensional probability density of displacements, which is obtained from 2D-Fourier transformation of the $\mathbf{q}$ space data, can be written as the product of the average propagator in the first time interval and a conditional probability function which possesses a different interpretation for each of the experiments due to the nature of how $\mathbf{q}$ space is sampled (see Eqs. [5] and [10]). VEXSY is characterized by two truly independent wave vectors $\mathbf{q}_1$ and $\mathbf{q}_3$, and Fourier transformation with respect to $\mathbf{q}_1$ and $\mathbf{q}_3$ leads to a plot of the two displacements which are defined by these wave vectors, namely $\mathbf{R}_1$ and $\mathbf{R}_3$. From Eq. [5] it can be seen that the conditional probability $\mathcal{P}_V(Z_1, \Delta \mid Z_3,\ \Delta;\ \tau_m)$, itself being a two-dimensional function, is obtained from dividing the 2D-probability density $S(Z_1, Z_3)$ by the propagator $\bar{P}(Z_1, \Delta)$,

$$\mathcal{P}_V(Z_1, \Delta \mid Z_3,\ \Delta;\ \tau_m) = S(Z_1, Z_3)/\bar{P}(Z_1, \Delta), \quad [18]$$

where the propagator itself is available via

$$\bar{P}(Z_1, \Delta) = \int S(Z_1, Z_3)\, dZ_3. \quad [19]$$

Examples for the interpretation of $\mathcal{P}_V(Z_1, \Delta \mid Z_3,\ \Delta;\ \tau_m)$ have been presented in (*19*). In SERPENT, Fourier transformation is performed with respect to $\mathbf{q}_2$ and $\mathbf{q}_3$ which render the corresponding displacements from the beginning of the sequence up to the application of the second and the third gradient pulse, respectively. The division can again be applied (see Eq. [10]), but the conditional probability $\mathcal{P}_S(\mathbf{R}_1, \Delta_1 \mid \mathbf{R}_2', \Delta_2)$ now relates displacements in interleaved time intervals (*16*).

It is quite obvious that under the conditions shown in Fig. 1c, both treatments should lead to equivalent results, the only difference being that VEXSY is performed by independent variation of the first and third gradient pulses, SERPENT by variation of the second and third gradient pulses. The formal equivalence of Eqs. [14] and [17] can be proved by reordering the SERPENT data in $\mathbf{q}$ space—as the condition $\mathbf{k}_1 + \mathbf{k}_2 + \mathbf{k}_3 = 0$ from the general case must be met, each point in (q_2, q_3) space can be transformed into a point in (q_1, q_3) space—and subsequent Fourier transformation with respect to the new variables. The equivalent operation in displacement space is to compute $S(Z_1, Z_2) = S(Z_1, Z_2' - Z_1)$ from each point in (Z_1, Z_2') space. Then Eq. [17] transforms into

$$\begin{aligned} S(Z_1, Z_2) &= \bar{P}(Z_1, \Delta_1)\mathcal{P}_V(Z_1, \Delta_1 \mid Z_2' - Z_1, \Delta_2 - \Delta_1;\ 0) \\ &= \bar{P}(Z_1, \Delta_1)\mathcal{P}_V(Z_1, \Delta_1 \mid Z_2,\ \Delta_2 - \Delta_1;\ 0), \end{aligned} \quad [20]$$

which is identical to Eq. [14] because $\Delta_1 = \Delta$ and $\Delta_2 = 2\Delta$.

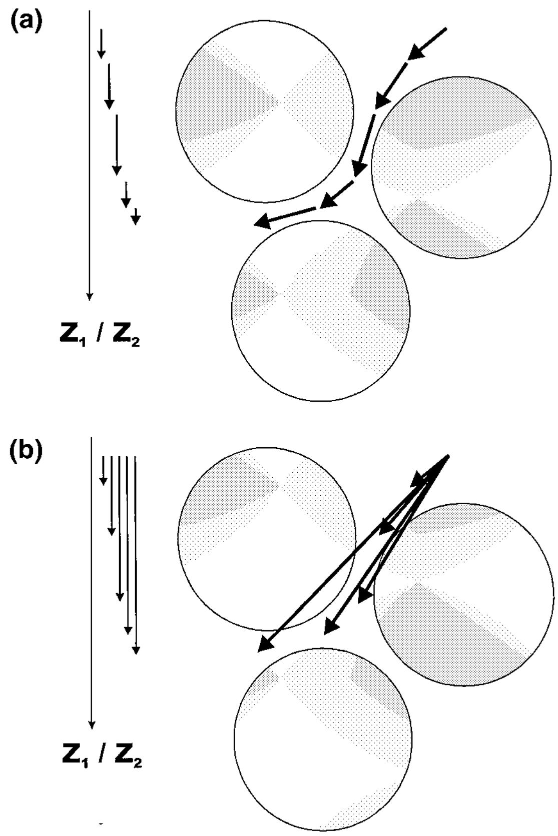

FIG. 2. Visualization of fluid flow through a model porous medium, symbolized by a packing of monodisperse spherical beads. The arrows represent displacements of a single molecule. (a) The particle's motion is split into a series of displacements, symbolized by arrows the starting point of which coincides with the end point of the previous arrow. Each arrow represents displacements during identical intervals, Δ. The components of these vectors parallel to the direction of net mass transport, Z, are indicated at the axis on the left-hand side of the figure. In VEXSY, the displacement during the first interval (Z_1, the projection of the first arrow) is measured along with the displacement during some later interval (Z_2, the projection of any other arrow) after a mixing time τ_m. (b) Same as in (a), but with each arrow now representing the total displacement from the particle's starting point for increasing times. In SERPENT, the displacement during the first interval Δ_1 (Z_1, the projection of the first arrow) is measured along with the total displacement during some longer interval Δ_2 (Z_2, the projection of any other arrow) where each interval begins at the same time.

INTERPRETATION OF INTEGRAL AND DIFFERENTIAL DISPLACEMENTS—EXPERIMENTAL CONSIDERATIONS

A comparison of the VEXSY and SERPENT sequences necessarily involves discussing their applicability to real systems and the interpretation of the results. It was shown that VEXSY compares spin displacements during two identical time intervals Δ with each other which are separated by a mixing time τ_m. It is frequently assumed that the measurement during Δ will provide a "snapshot" of the velocity field and that Δ is chosen sufficiently short to prevent mixing of spin velocities; VEXSY thus stresses the aspect of *differential* displacements, which correspond to velocities, hence the original term "velocity exchange spectroscopy." This fact is illustrated in Fig. 2a for a typical application of multigradient PFG experiments, laminar flow around spherical particles. The motion of fluid particles is shown symbolically by a train of straight arrows; the projection of these displacement arrows onto one axis is measured by the choice of the direction of the pulsed field gradient. By treating τ_m as a variable and increasing it stepwise between experiments, starting with $\tau_m = 0$, one successively correlates the first and the second arrow; the first and the third arrow; the first and the fourth arrow, and so forth. An average over fast and slow spins is taken and the correlation is found to decrease as the final displacement becomes more and more independent from the initial displacement.

In SERPENT, on the other hand, one compares spin displacements during an initial encoding time interval, Δ_1, with those during a much longer time interval Δ_2 incorporating Δ_1. One therefore stresses the aspect of *integral* displacements as is shown in Fig. 2b. By stepwise increasing Δ_2, which now takes the place of τ_m, each spin adds a further distance to the one initially traveled during Δ_1. From the fact that—for the presented abstract model in the absence of backflow—displacements are steadily increasing it can be understood easily that correlations between integral quantities (as derived from SERPENT experiments) decay much slower (*19*) than those between differential ones (as obtained from VEXSY).

The above-mentioned possibility of constructing a plot of $S(Z_1, Z_2' - Z_1)$ from the SERPENT data does not necessarily provide better insight into the flow properties as in this case, displacements in two successive time intervals are compared to each other, in particular when the second is much longer than the first one. Such a case is identical to an "asymmetric" VEXSY experiment with $\tau_m = 0$ and different encoding intervals, a situation where velocities averaged over different times are to be compared to each other, which would normally not find suitable applications.

From the experimental point of view, SERPENT is to be preferred when the evolution of displacement probabilities over time and their dependence on a starting distribution are of interest. The possibility of setting the condition $\Delta_2 = \Delta_1$ (i.e., the second and third gradient pulses superposed) then provides a well-defined reference point of perfect correlation between displacements Z_1 and Z_2'. VEXSY, on the other hand, is the method of choice when velocities are to be compared with each other and the "history" of displacements during the mixing time τ_m is not directly measured. Note that even for $\tau_m = 0$, velocities are allowed to change during an interval Δ and that in general, a perfect correlation between the measured quantities Z_1 and Z_2 cannot be achieved. The proper choice of the initial encoding interval might be crucial for the interpretation of both experiments in the case of flow investigations. One can only discuss a "snapshot" of the velocity field if the encoding time is short compared to the timescale of velocity change. On the other hand, a too short encoding time leads to a reduced correlation between the measured displacement vectors if small-scale random motions such as self-diffusion are similar in magnitude to the displacement contributions from coherent motion.

CONCLUSIONS

We have compared two different multidimensional pulsed field gradient sequences which have the purpose of correlating spin displacements in different time intervals with each other. The simplest possible sequence, three-pulse SERPENT, correlates initial displacements with integral displacements by encoding two interleaved time intervals beginning with the first gradient pulse. It is suggested for diffusion or flow problems where the dependence of the long-time, integral displacement statistics on the initial conditions is of primary interest. VEXSY, on the other hand, correlates two differential quantities, i.e., initial and final displacements. The experiment consists of four pulses stepped in two pairs separated by a mixing time, where no information about displacements during this mixing time is retained. VEXSY is frequently applied when instantaneous velocities and their change with time are to be investigated. Both sequences can be described by equivalent formalisms which allow the representation of the evolution of displacements by means of conditional probabilities.

REFERENCES

1. P. T. Callaghan and B. Manz, *J. Magn. Reson. A* **106,** 260 (1994).
2. J. Jeener, B. H. Meier, P. Bachmann, and R. R. Ernst, *J. Chem. Phys.* **71,** 4546 (1979).
3. R. R. Ernst, G. Bodenhausen, and A. Wokaun, "Principles of Nuclear Magnetic Resonance in One and Two Dimensions," Clarendon, Oxford (1987).
4. K. Schmidt-Rohr and H. W. Spiess, "Multidimensional Solid-State NMR and Polymers," Academic Press, London (1994).
5. E. O. Stejskal and J. E. Tanner, *J. Chem. Phys.* **42,** 288 (1965).
6. P. T. Callaghan, "Principles of Nuclear Magnetic Resonance Microscopy," Clarendon, Oxford (1991).
7. B. Blümich, "NMR Imaging of Materials," Oxford Univ. Press, Oxford (2000).
8. S. Han and B. Blümich, *Appl. Magn. Reson.* **18,** 101 (2000).
9. S. Han, S. Stapf, and B. Blümich, *J. Magn. Reson.* **146,** 169 (2000).
10. P. P. Mitra, *Phys. Rev. B* **51,** 15074 (1995).
11. D. G. Cory, A. N. Garroway, and J. B. Miller, *Polym. Preprints* **31,** 149 (1990).
12. Y. Cheng and D. G. Cory, *J. Am. Chem. Soc.* **121,** 7935 (1999).
13. P. T. Callaghan, S. L. Codd, and J. D. Seymour, *Concepts Magn. Reson.* **11,** 181 (1999).
14. S. L. Codd, B. Manz, J. D. Seymour, and P. T. Callaghan, *Phys. Rev. E* **60,** R3491 (1999).
15. A. Caprihan and J. D. Seymour, *J. Magn. Reson.* **144,** 96 (2000).
16. S. Stapf, R. A. Damion, and K. J. Packer, *J. Magn. Reson.* **137,** 316 (1999).
17. S. Stapf and K. J. Packer, *Appl. Magn. Reson.* **15,** 303 (1998).
18. J. Kärger and W. Heink, *J. Magn. Reson.* **51,** 1 (1983).
19. S. Stapf and B. Blümich, *Magn. Reson. Imaging* **19,** 385 (2001).